Theoretical Study of the Twisted Intramolecular Charge Transfer in 1-Phenylpyrrole

Boris Proppe[†]

Institut für Chemie-Physikalische und Theoretische Chemie, Freie Universität Berlin, Takustrasse 3, D-14195 Berlin, Germany

Manuela Merchán*[,‡]

Departamento de Química Física, Universitat de València, Dr. Moliner 50, Burjassot, E-46100 Valencia, Spain

Luis Serrano-Andrés[§]

Department of Theoretical Chemistry, Chemical Centre, P.O. Box 124, S-221 00 Lund, Sweden

Received: October 12, 1999

Ab initio results for the electronic spectra of 1-phenylpyrrole are presented. Vertical, emission, and nonvertical excitation energies have been computed using multiconfigurational second-order perturbation theory by means of the CASPT2 method. In the S_0 and S_1 states the most stable conformation was determined to be a twisted structure with a dihedral angle between the planes of the rings of 41.4° and 25.5°, respectively. The most intense feature of the absorption spectrum is predicted to be the S_0 (1^1A) → S_1 (2^1A) transition placed in vacuo at 5.07 eV. The lowest-excited state, S_1 (1^1B), identified as the "locally excited" (LE) state, is calculated in vacuo to lie vertically 4.39 eV above the ground state, with the position of the 0-0 transition at 4.16 eV and a fluorescence maximum of 4.07 eV. An additional fluorescence feature is found at 3.72 eV in acetonitrile from a "twisted intramolecular charge transfer" (TICT) state in a perpendicular conformation. The absence of the low-energy emission in vacuo is rationalized in terms of the different shapes of the S_0 and S_1 hypersurfaces. From the overall study it is concluded that the 1-phenylpyrrole system can be considered as an example where the TICT occurs.

1. Introduction

Photoinduced intramolecular charge transfer (ICT) states of organic compounds play a fundamental role in many processes of current interest.[1] In a large number of molecules, the occurrence of an ICT state is related to the observation of two distinct fluorescence bands, the so-called dual fluorescence. In addition to a "normal" fluorescence band (B fluorescence), involving a "locally excited" (LE) state, a red-shifted emission (A fluorescence) is observed in polar solvents attributed to an ICT state.[2,3]

The concept of twisted intramolecular charge transfer (TICT) state[2] has been especially useful to rationalize unexpected fluorescence features of many compounds. The 4-(*N*,*N*-dimethylamino)benzonitrile (DMABN) can probably be considered the most well-known TICT example. The TICT state was suggested originally to be reached by internal rotation in the excited state around a single bond towards the perpendicular geometry. Nevertheless, several alternative mechanisms (involving the inversion mode of the nitrogen in the dimethylamino group, the bending mode of the cyano group, etc.) have been recently discussed to explain the observed dual fluorescence phenomenon in DMABN.[3−7] The TICT model has been adopted for donor−acceptor biaryls, where the stabilization of the ICT state is supposed to be achieved at the perpendicular orientation of the arylic moieties.[8] The present investigation has been focused on the 1-phenylpyrrole (PHPY) system, archetype of this class of compounds, which shows dual fluorescence in polar solvents.[9] Compared to DMABN, the dimensionality of the problem is considerably reduced in PHPY. The torsional motion of the two aromatic groups connected by a single bond is the only possible promoting mode in order to reach an ICT state. Whether it is a TICT state or not would depend, however, on the relative location of the hypersurfaces involved. Several ICT and TICT states might contribute to the observed A fluorescence in polar solvents.

PHPY has been the subject of several previous studies.[8−14] Theoretical work has been carried out at the semiempirical level (see, e.g., refs 12 and 14). To the best of our knowledge, the most recent experimental data come from the electronic spectra of jet-cooled PHPY reported by Okuyama et al.[11] The most stable conformation for the ground state (S_0) has been determined to be a twisted form with a dihedral angle of 38.7°. The S_1 state has also a twisted form, with a somewhat smaller dihedral angle (19.8°), and the 0-0 transition observed at 4.40 eV. In addition, for jet-cooled PHPY, the deduced barrier heights to planarity and to perpendicularity indicate that the electronic excitation makes the system to be more rigid to torsion.[11] No indication of TICT has appeared on the shape of the S_1-state torsional potential determined by Okuyama et al.[11] These authors made the assumption that the lowest-energy band is composed of a single electronic transition. As discussed below, this is not actually the case. The 0-0 transition determined by Okuyama et al. does not correspond to the electronic transition responsible

[†] E-mail: boris@fu-berlin.de.
[‡] E-mail: Manuela.Merchan@UV.es.
[§] E-mail: Luis.Serrano@UV.es. Present address: Departamento de Química Física, Universitat de València, Dr. Moliner 50, Burjassot, E-46100 Valencia, Spain.

10.1021/jp993627g CCC: $19.00
Published on Web 02/01/2000

for the spectroscopic feature with maximum intensity in the lowest-energy region of the absorption spectrum.

Earlier spectroscopic and photophysical studies of PHPY are also available.[9] The absorption spectra have a broad absorption band in the energy range 4.4−5.5 eV, which shows a bathochromic effect on going from the vapor to solution. At 300 K, the maximum of the band has been placed at 5.03 eV (4.86 eV at 294 K[11]) in the vapor, 4.86 eV in *n*-heptane, and 4.90 eV in acetonitrile.[9] In 1-phenylpyrazole, a closely related system to PHPY, a shoulder has been detected at 4.35 eV in a nonpolar solvent, which is submerged under the broad absorption envelope in polar media. Based on these observations, Sarkar and Chakravorti[9] have suggested the presence of a hidden band under the broad curve of the strong band of PHPY, similar as in the biphenyl molecule. The present results confirm a weak transition below the main feature of the broad band. PHPY exhibits dual fluorescence in polar solvents. For instance, the emission maxima in acetonitrile have been recorded at 3.65 eV (A fluorescence) and 4.05 eV (B fluorescence). The latter is not significantly affected by the nature of the solvent (4.08 eV in *n*-heptane).

From this brief summary, one can easily conclude that the assignment of the spectrum of PHPY is still under debate. There are a number of open questions related to it. Can theoretical calculations confirm the geometry derived experimentally for the ground state? What type of hypersurfaces can be expected for the excited states? And, a key question: is PHPY a TICT problem? In order to clarify some aspects of the controversial issues mentioned above related to the electronic structure, geometry, and spectral features of PHPY, a comprehensive theoretical ab initio study has been carried out. The results derived from the investigation are presented here. The main features of the absorption spectrum have been characterized and analyzed. The study includes geometry determination of the ground state, considering the main conformations of PHPY (coplanar, twisted, and perpendicular). Geometries of selected excited states, which are relevant for the understanding of the spectroscopic behavior of the PHPY system, have been also characterized. It made possible the computation of non-vertical and emission transition energies for certain states, including the most plausible candidates to ICT states.

The study has been performed at the CASSCF/CASPT2 level. In this way, the most important reorganization and correlation effects in the valence shell are accounted for by using the CASSCF method.[15] The remaining correlation contributions are considered within the framework of multiconfigurational second-order perturbation theory, the CASPT2 approach.[16,17] The successful performance of the CASPT2 method in computing differential correlation effects for excitation energies has been illustrated in a number of earlier applications (see, e.g., refs 18−20). Particularly connected to the present study are the investigations carried out on the ICT process process in aminobenzonitriles,[21] on the internal rotational barrier of biphenyl,[22] and on the electronic spectra of biphenyl,[23] biphenyl cation, and anion.[24]

The paper is organized as follows. Computational details are described in the next section. Following, the internal rotational barrier heights for ground-state PHPY are characterized. Results and analysis on the computed absorption spectrum are subsequently considered, together with the emission maxima obtained for the fluorescence features, the corresponding 0-0 transitions, and comparisons to previous findings. Our conclusions and answers to the questions rising from the discussion above are summarized in the last section.

2. Details of Calculations

Generally contracted basis sets of atomic natural orbital (ANO) type were employed, which were obtained from the C,N-(14s9p4d)/H(8s) primitive sets.[25] These basis sets were designed to optimally treat correlation and polarization effects. The contraction scheme C,N[3s2pld]/H[2s] was used. In order to characterize the lowest Rydberg states, the basis set was supplemented with two s- and two p-type diffuse functions placed at the center of the molecule (see exponents elsewhere[26]). The basis set is the same as was used in previous studies of electronic spectra of organic compounds of similar molecular size like PHPY (see, e.g., naphthalene,[26] biphenyl,[23] and *trans*-stilbene[27]). As discussed in these papers, the basis set is able to describe the excited states with enough flexibility to achieve the required accuracy at a moderate computational cost.

The PHPY molecule is located with the long molecular axis corresponding to the *z* axis. For coplanar PHPY the molecule is placed in the *yz* plane. The π orbitals then belong to the b_1 and a_2 irreducible representations of the C_{2v} symmetry point group. For perpendicular PHPY the pyrrolic group is placed in the *yz* plane. The geometry of ground-state PHPY was fully optimized, within the C_{2v} symmetry constraints for the coplanar and perpendicular conformations, and within the C_2 symmetry for the twisted structure. The π-CASSCF level wave functions (11 active π orbitals/12 π active electrons) were used for the geometry optimizations employing the ANO-type C,N[3s2p1d]/H[2s] basis sets. The remaining electrons were kept inactive. The calculations comprise 172 basis functions, involving 743 primitive functions. The number of degrees of freedom in the geometry optimizations were of 26 and 19 for the C_2 and C_{2v} symmetries, respectively. Several excited states were also optimized at the same level of theory. The optimized structures for the ground state at the π-CASSCF level were used to calculate the internal rotational barrier heights. The π-CASSCF molecular geometries of PHPY in twisted, coplanar, and perpendicular conformations were used to obtain the corresponding vertical electronic transitions. In order to include the dynamical correlation effects, the π-CASSCF wave functions were employed as reference functions in the second-order perturbation treatment through the CASPT2 method.[16,17]

Initially, the vertical spectrum was computed employing the π-valence active space. Due to the presence of relatively strong intruder states in certain cases, the active space was enlarged to 13 MOs (with 12 active electrons), *ext*-CASSCF hereafter, including an extra active orbital of π nature in two different irreducible representations of the C_2 (C_{2v}) symmetry group. Additional intruder states weakly interacting with the reference *ext*-CASSCF wave function were treated using the level-shift technique (LS-CASPT2).[19,28,29] Calibration calculations for PHPY obtained with a level-shift parameter within the range 0.1−0.4 au show that at 0.3 au the intruder states are effectively removed for all the states of interest. Therefore only results with the level-shift parameter of 0.3 au are reported here.

The molecular orbitals (MOs) for the excited states computed vertically were obtained from average CASSCF calculations, where the averaging includes all states of interest of a given symmetry. The number of the states included in the state average CASSCF calculations, together with the number of configurations in the CASSCF wave functions, details on the active spaces used, and the type of valence states computed are given in Table 1. The ordering of the states included corresponds to the one obtained vertically at the LS-CASPT2 level. The energy of each excited state is referred to a ground-state energy computed with

TABLE 1: CASSCF Wave Functions used for 1-Phenylpyrrole[e]

wave function	states	no. of conformations[c]	N^{d}_{states}
C_{2v} Coplanar[a] (No. of Occupied SCF MOs: 19, 4, 13, 2)			
π-CASSCF (inactive: 19; 0; 13; 0) (active: 0; 7; 0; 4)			
	1^1A_1	30632	1
ext-CASSCF (inactive: 19; 0; 13; 0) (active: 0; 8; 0; 5)			
	1^1A_1, 2^1A_1, 3^1A_1, 4^1A_1	368532	4
	1^1B_2, 2^1B_2	367632	2
C_2 twisted[b] (No. of Occupied SCF MOs: 21, 17)			
π-CASSCF (inactive: 19, 13) (active: 4, 7)			
	1^1A	30632	1
ext-CASSCF (inactive: 19, 13) (active: 5, 8)			
	1^1A, 2^1A, 3^1A, 4^1A	368532	4
	1^1B, 2^1B	367632	2
C_{2v} Perpendicular[a] (No. of Occupied SCF MOs: 19, 9, 8, 2)			
π-CASSCF (inactive: 19, 7, 6, 0) (active: 0, 3, 4, 4)			
	1^1A_1	15512	1
ext-CASSCF (inactive: 19, 7, 6, 0) (active: 0, 3, 5, 5)			
	1^1A_1,2^1A_1,3^1A_1	185382	3
	1^1B_1	184482	2
	1^1B_2	183150	1
	1^1A_2	183150	1

[a] Within parentheses the number of orbitals of the symmetries: a_1, b_1, b_2, a_2 of the point group C_{2v}. [b] Within parentheses the number of orbitals of symmetry a and b of the point group C_2. [c] Number of configurations in the CASSCF wave functions. [d] States included in the average CASSCF calculation. [e] The geometry optimizations have been performed at the π-CASSCF level (11 active orbitals/12 active electrons). The spectra have been computed using the extended CASSCF wave function (*ext*-CASSCF, 13 active orbitals/12 active electrons).

the same active space. All electrons except the *cores* were correlated at the second-order level.

For the singlet−singlet dipole-allowed transitions, the oscillator strength in the dipole length form f^L was considered,

$$f^L = \frac{2}{3}|M_{ij}|^2 \Delta E$$

where the dipole transition moment M_{ij} and the energy difference ΔE involving the ground and excited states are expressed in atomic units. The M_{ij} values were computed using the CASSCF state interaction (CASSI) method.[30,31] ΔE was replaced by the energy difference obtained at the LS-CASPT2 level. The combined use of the CASSI and CASPT2 methods to determine oscillator strengths is by now a well-established approach in the study of electronic spectra of organic compounds.[18−20]

The solvation effects on excitation energies have been studied by using a self-consistent reaction field (SCRF) method[32] where the solvent is simulated by an external continuum with a dielectric constant ϵ surrounding a spherical cavity which contains the molecule. The molecule polarizes the solvent and induces an electric field which interacts with the solute. The solute−solvent interaction is then added as a perturbation of the Hamiltonian of the free solute and the wave function is determined iteratively. Equilibrium between the electronic state of the solute and the reaction field is assumed, but in excitation or emission processes the relaxation of the reaction field may be incomplete. Therefore, the time dependence of the absorption process has been accounted for by partitioning the reaction field factor into inertial (slow motion: nuclei) and optical (fast motion: electrons) components. The inertial component is determined from the initial state properties and kept fixed for the calculation of the reaction field of the final state, where only the optical component is optimized until self-consistency. The optical component can be considered as the instantaneous electronic polarization that follows the promotion of a photon and is in a first approximation proportional to the dielectric constant at infinite frequency ϵ^∞, where $\epsilon^\infty = n^2$, and n is the refractive index of the solvent. In the present study all the reaction fields have been determined at the CASSCF level and added as an external perturbation to the zeroth-order Hamiltonian of the CASPT2 method[32] (CASSCF-RF/CASPT2). Cavity radii of 8.30 and 8.61 au have been used for the molecule in the twisted and perpendicular conformations, respectively. They have been obtained adding to the molecular size the van der Waals' radius of hydrogen (1.2 Å). A dielectric constant $\epsilon = 38.8$ and a refraction index of 1.1746 have been used as parameters to simulate acetonitrile as a solvent. The basis sets, geometries, and active spaces were the same as those used for the isolated molecule.

All calculations were performed with the MOLCAS-4 quantum chemistry software.[33]

3. Results and Discussion

The relative location of the excited states with respect to the ground state in different parts of the complex hypersurface is of importance to rationalize the spectroscopic behavior of the PHPY system. As a preliminary step towards the theoretical understanding of the electronic spectrum of PHPY, the geometry for the ground state and its internal rotational barrier are first considered. Vertical, emission, and nonvertical transition energies are next analyzed. Furthermore, the present findings will be compared with previous theoretical results and available experimental data.

3.1. Ground-State Geometry Determinations. The optimized geometrical parameters obtained at the π-CASSCF level, employing the ANO C,N[3s2pld]/H[2s] basis set, are given in Figure 1. The dihedral angle (θ) between the phenyl (PH) and pyrrolic (PY) planes corresponds to 0° and 90° for the coplanar and perpendicular conformations, respectively. Total and relative energies computed for the optimal structures of coplanar, twisted, and perpendicular ground-state PHPY are listed in Table 2. The relative stability among the different conformers of biaryls is usually discussed in terms of the balance between *ortho*-hydrogen repulsion and strength in π-electron conjugation. If the latter dominates over the former the most stable conformation is planar. Otherwise, the molecule has an nonplanar structure. As can be seen in Figure 1, the most significant geometrical changes take place in those parameters involved in determining the distance between the hydrogen atoms in *ortho* position. Thus, the perpendicular structure, where the π-electron conjugation is less favored, has the largest value of the interannular C−N bond distance. In addition, the smallest $C-H_{ortho}$ bond distance and the largest $N-C_{PH}-C_{PH}$ angle are found for planar PHPY, which reflects the steric repulsion between the *ortho* hydrogen atoms. It is decreased in the twisted structure, allowing the interring C−N bond distance to become slightly shorter. An enlargement of the central bond length is noted on going from the twisted to the perpendicular structure, where both π-electron conjugation and *ortho*-hydrogen repulsion are drastically decreased. Accordingly, the C−C bond distances of the phenyl group become progressively more equalized during the twisting process from $\theta = 0°$ to $\theta = 90°$.

The most stable conformation is computed to be a twisted form (cf. Table 2) in agreement with the most recent experimental determination.[11] The computed rotational angle for the equilibrium geometry of 1-phenylpyrrole (41.1°) is similar to that obtained in biphenyl (44.3°), which was also optimized at

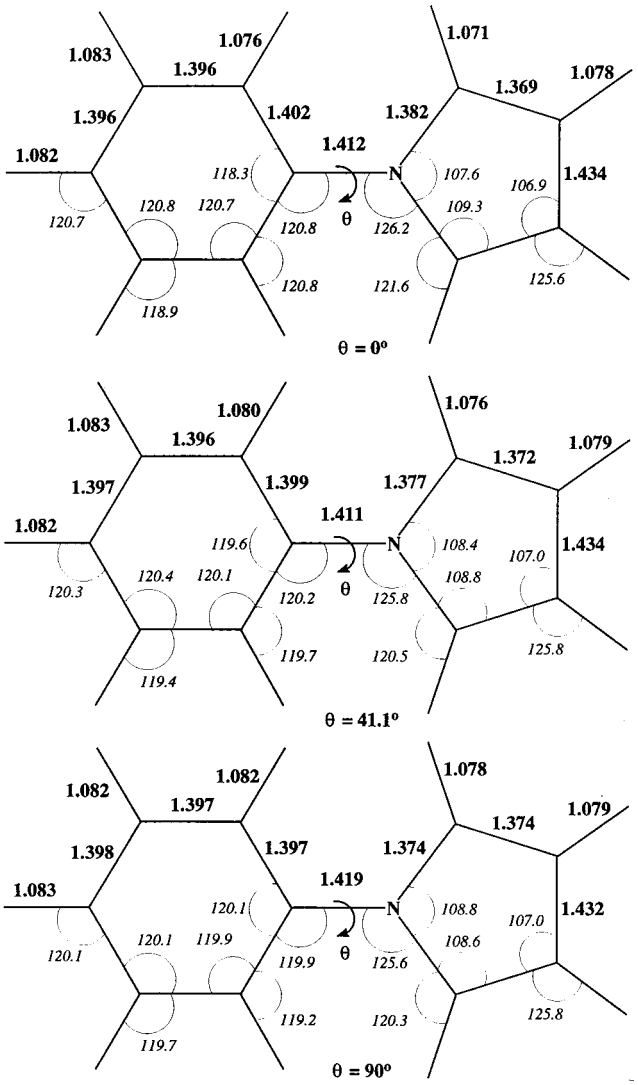

Figure 1. Geometries optimized at the π-CASSCF level for ground-state NPP. The dihedral angle between the phenyl and pyrrolic planes is denoted by θ. The coplanar form corresponds to $\theta = 0°$ and the perpendicular structure to $\theta = 90°$. Bond lengths in angstroms and angles in degrees.

TABLE 2: Total Energies (E_t) and Relative Energies (E_r) Computed for the Ground State of 1-Phenylpyrrole Employing the π-CASSCF Optimized Geometries[a]

	CASSCF		CASPT2	
structure	E_t (au)	E_r (eV)	E_t (au)	E_r (eV)
coplanar (1^1A_l)	−438.543 628	0.071	−439.831 462	0.101
twisted (1^1A)	−438.546 231	0.000	−439.835 162	0.000
perpendicular (1^1A_1)	−438.544 314	0.052	−439.832 805	0.064

[a] The π-valence active space (with the π-valence electrons active) was employed.

the π-CASSCF level.[22] The highest level of theory yields 0.1 eV (9.73 kJ/mol) and 0.064 eV (6.20 kJ/mol) for the barrier heights at 0° and 90°, respectively. A larger barrier height to planarity (12.93 kJ/mol) than to perpendicularity (6.40 kJ/mol) was also found for biphenyl.[22]

The results for PHPY can be compared with the data reported by Okuyama et al.,[11] obtained from jet-cooled spectroscopic studies. The computed result for the dihedral angle (41.1°) is consistent with the datum derived experimentally (38.7°). The torsional potential obtained by Okuyama et al. led to the reverse trend for the barrier height of the planar and perpendicular forms, 5.47 and 8.96 kJ/mol, respectively. The one-dimensional torsional potential with respect to the dihedral angle[11] might be sensitive to the fitting procedure, leading to either an underestimation or an overestimation of the barrier heights, in a similar way as it does occur in biphenyl (see discussion in ref 22). In order to rationalize the apparent discrepancy between theory and experiment, it is worth keeping in mind that a multidimensional treatment, i.e., full geometry optimization has been here carried out for the three conformers. The reported geometries optimized at the CASSCF level have been used in the computation of the vertical transition energies.

TABLE 3: Computed CASSCF and CASPT2 Excitation Energies (eV), Related Oscillator Strengths, and CASSCF Dipole Moments (μ, D) for the Vertical Excited States of Coplanar, Twisted, and Perpendicular 1-Phenylpyrrole

state	CASSCF	CASPT2	oscillator strength	μ
coplanar				
1^1A_1				−1.112
1^1B_2	4.96	4.30	0.002	−0.470
2^1A_1	5.68	4.80	0.225	2.897
2^1B_2	6.32	5.25	0.007	6.561
3^1A_1	6.66	5.56	0.257	9.042
4^1A_1	7.28	6.03	0.145	1.233
twisted				
1^1A				−1.509
1^1B	5.17	4.39	0.001	−1.004
2^1A	6.05	5.07	0.263	3.100
2^1B	6.42	5.30	0.006	8.513
3^1A	6.35	5.61	0.011	10.753
4^1A	7.16	5.90	0.114	2.613
perpendicular				
1^1A_1				−2.042
1^1B_1	5.35	4.59	0.002	−2.845
2^1B_1	6.28	5.35	0.000	11.008
2^1A_1	6.13	5.45	0.005	4.880
3^1A_1	6.84	5.82	0.070	5.280
1^1A_2	6.04	5.89	forb.	10.107
1^1B_2	7.66	6.02	0.173	−2.464

3.2. Vertical Transition Energies. A number of calculations were first carried out at the coplanar geometry of ground-state PHPY to characterize the energy range of the low-lying Rydberg states. For computing the lowest Rydberg transition the π-valence active space was enlarged with a 3s Rydberg orbital. The lowest Rydberg state $^1B_1(3s)$ described mainly by the one-electron promotion from the highest occupied molecular orbital (HOMO), $4b_1$ MO, to a 3s Rydberg orbital, was found at 5.53 eV above the ground state (CASPT2 result). It is close to the excitation energy obtained for the analogous state in biphenyl, 5.60 eV.[23] In a similar way, the 3p Rydberg states were computed to lie around 6 eV. Consequently, the study of the singlet-singlet electronic spectrum involving valence excited states was focused on the energy region below 6 eV. The results for the vertical excitation energies computed for PHPY are collected in Table 3, where the first column labels the state, the second and third columns give the vertical transition energies obtained by the CASSCF (*ext*-CASSCF) and CASPT2 (LS-CASPT2) calculations (see previous section), respectively, and then the oscillator strength and dipole moments are compiled.

The relative energy of each excited state refers to the ground state energy computed with the same active space at the same conformation (coplanar, twisted, perpendicular). Detailed information about the *ext*-CASSCF wave functions of the singlet excited states considered is given in Table 4.

In order to obtain further insight into the nature and evolution of the excited states upon the internal rotation, the structure and SCF orbital energies of the main π MOs involved in the description of the low-lying valence singlet excited states are shown in Figures 2 and 3.

TABLE 4: *ext*-CASSCF Wave Functions for 1-Phenylpyrrole: Principal Configurations, Weights, and Number (weights) of Singly (S), Doubly (D), and Triply (T) Excited Configurations[a] with Coefficients Larger than 0.05

			no. of configurations (weights)		
state	principal configurations	%	S	D	T
coplanar					
1^1A_l	$...(3b_1)^2(1a_2)^2(2a_2)^2(4b_1)^2$	79.2	1 (1.7%)	18 (9.3%)	
1^1B_2	$(4b_1)\rightarrow(3a_2)$	43.8	5 (69.7%)	12 (14.0%)	4 (1.5%)
	$(1a_2)\rightarrow(5b_1)$	22.8			
2^1A_1	$(4b_1)\rightarrow(5b_1)$	50.6	7 (72.3%)	15 (9.3%)	2 (1.4%)
	$(2a_2)\rightarrow(3a_2)$	12.4			
2^1B_2	$(2a_2)\rightarrow(5b_1)$	70.3	4 (72.8%)	15 (12.0%)	5 (2.1%)
3^1A_1	$(2a_2)\rightarrow(3a_2)$	55.3	4 (68.7%)	15 (13.8%)	5 (1.7%)
	$(4b_1)\rightarrow(5b_l)$	10.5			
4^1A_1	$(3b_1)\rightarrow(5b_1)$	19.0	5 (61.5%)	15 (18.9%)	5 (2.2%)
	$(2a_2)\rightarrow(4a_2)$	17.5			
	$(4b_1)\rightarrow(6b_1)$	13.7			
twisted					
1^1A	$... (16b)^2(20a)^2(17b)^2(21a)^2$	78.7	2 (2.5%)	19 (10.0%)	
1^1B	$(17b)\rightarrow(23a)$	42.6	3 (69.9%)	15 (14.5%)	6 (3.3%)
	$(20a)\rightarrow(18b)$	26.7			
2^1A	$(17b)\rightarrow(18b)$	57.9	6 (71.0%)	15 (11.9%)	2 (1.9%)
	$(21a)\rightarrow(26a)$	8.8			
2^1B	$(21a)\rightarrow(18b)$	74.5	1 (74.5%)	16 (11.0%)	8 (4.1%)
3^1A	$(21a)\rightarrow(23a)$	72.5	3 (74.1%)	18 (12.3%)	7 (2.5%)
4^1A	$(17b)\rightarrow(21b)$	33.1	7 (66.9%)	18 (14.6%)	8 (3.1%)
	$(21a)\rightarrow(26a)$	16.1			
perpendicular					
1^1A_1	$...(8b_2)^2(1a_2)^2(9b_1)^2(2a_2)^2$	80.3	1 (0.8%)	11 (13.4%)	
1^1B_1	$(1a_2)\rightarrow(9b_2)$	37.3	4 (72.5%)	9 (15.8%)	9 (4.0%)
	$(8b_2)\rightarrow(3a_2)$	32.4			
2^1B_1	$(2a_2)\rightarrow(9b_2)$	77.2	3 (79.4%)	10 (7.6%)	9 (5.8%)
2^1A_1	$(2a_2)\rightarrow(3a2)$	45.6	4 (73.7%)	16 (13.0%)	11 (4.4%)
	$(9b_1)$-$(11b_1)$	18.0			
3^1A_1	$(2a_2)\rightarrow(3a_2)$	32.8	3 (70.9%)	14 (13.9%)	11 (4.6%)
	$(9b_1)\rightarrow(11b_l)$	22.0			
	$(2a_2)\rightarrow(4a_2)$	16.1			
1^1A_2	$(9b_1)\rightarrow(9b_2)$	79.1	1 (79.1%)	10 (8.1%)	10 (5.3%)
1^1B_2	$(2a_2)\rightarrow(11b_l)$	80.0	3 (84.2%)	3 (2.0%)	12 (7.3%)

[a] With respect to the ground-state principal configuration.

Due to symmetry constraints, the *ext*-CASSCF natural orbitals and the π canonical SCF MOs are topologically equivalent. Thus, the effect of the twist angle on the computed excitation energies can be rationalized considering the principal configurations in the description of the excited states listed in Table 4, in terms of the *ext*-CASSCF natural orbitals, in conjunction with the evolution of the SCF orbital energies of the topologically equivalent MOs.

Three electronic transitions are found vertically in the energy range 4.4−5.3 eV for twisted PHPY. Transition from the ground state to the 2^1A state, placed at 5.07 eV with an oscillator strength of 0.26, can be related to the maximum of the lowest energy absorption band recorded around 5 eV in the vapor.[9,11] The *ext*-CASSCF wave function of the 2^1A state is mainly described by the singly excited configuration (17b → 18b) with weight 58%. The 2^1A state can be correlated with the 2^1A_1 (coplanar) and 1^1A_2 (perpendicular) states, which are computed at 4.80 and 5.89 eV, respectively. The orbital energy difference between the pair $5b_1-4b_l$ decreases by 0.44 eV with respect to the pair 18b−17b. The spacing between the $9b_2-9b_1$ increases, however, by 0.91 eV. In accordance with the predictions based on elementary MO theory, the electronic transition $1^1A \rightarrow 2^1A$ is lowered by 0.3 eV at the coplanar structure and is pushed up by 0.8 eV at the perpendicular conformation. It is worth mentioning the pronounced increase of the dipole moment for the 1^1A_2 (perpendicular) state. The one-electron promotion ($9b_1 \rightarrow 9b_2$) (weight 79%) characterizes the 1^1A_2 state. As can be seen in Figure 3, the $9b_1$ and $9b_2$ MOs are localized on the pyrrolic and the phenyl moieties, respectively. The charge transfer (CT) nature of the 1^1A_2 state explains its relatively large dipole moment compared to the ground state.

The computation clearly predicts an electronic transition with a small oscillator strength below the absorption maximum for twisted PHPY. It involves the 1^1B state, located at 4.39 eV, which correlates with the states 1^1B_2 (4.30 eV) and 1^1B_1 (4.59 eV) for the coplanar and perpendicular rotamers. The states are mainly described by two singly excited configurations (cf. Table 4). The orbital energies of the corresponding one-electron functions do not significantly change along the torsional reaction coordinate. Accordingly, the excitation energy keeps within 0.2 eV. The shoulder observed for 1-phenylpyrazole at 4.35 eV in a nonpolar solvent can be related to the computed $1^1A \rightarrow 1^1B$ electronic transition. The present results confirm, therefore, the presence of a hidden feature below the lowest energy broad band of PHPY, which was previously suggested by Sarkar and Chakravorti.[9] In addition, as shall be discussed below, the 1^1B state represents the most suitable candidate as source of the "normal" fluorescence.

The 2^1B and 3^1A excited states of twisted PHPY have large dipole moments, in accordance with the charge transfer character of the principal configurations describing the states (21a → 18b, 75%) and (21a → 23a, 73%), respectively. The 2^1B state is thus described mainly by the one-electron promotion from the HOMO to the lowest unoccupied molecular orbital (LUMO). As occurs in many organic systems, including biphenyl and stilbene, the (HOMO → LUMO) state is not the lowest excited state, as could be inferred from elementary MO theory. The 2^1B state, which is calculated to lie vertically 0.91 eV above

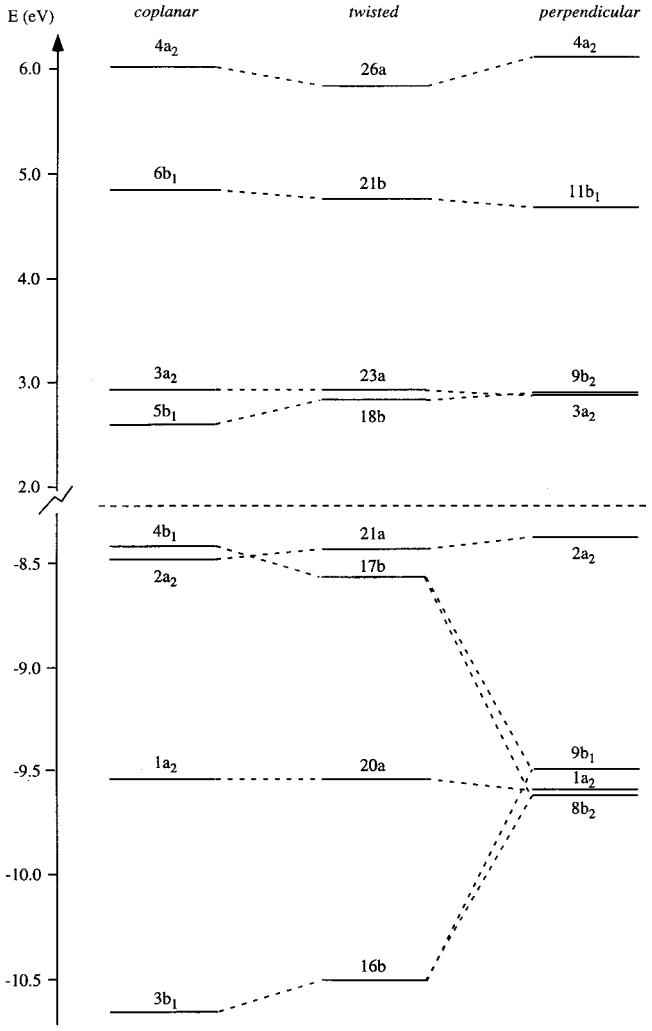

Figure 2. Schematic diagram showing the orbital distribution for the highest four occupied and lowest four unoccupied π MOs of coplanar, twisted, and perpendicular *N*-phenylpyrrole.

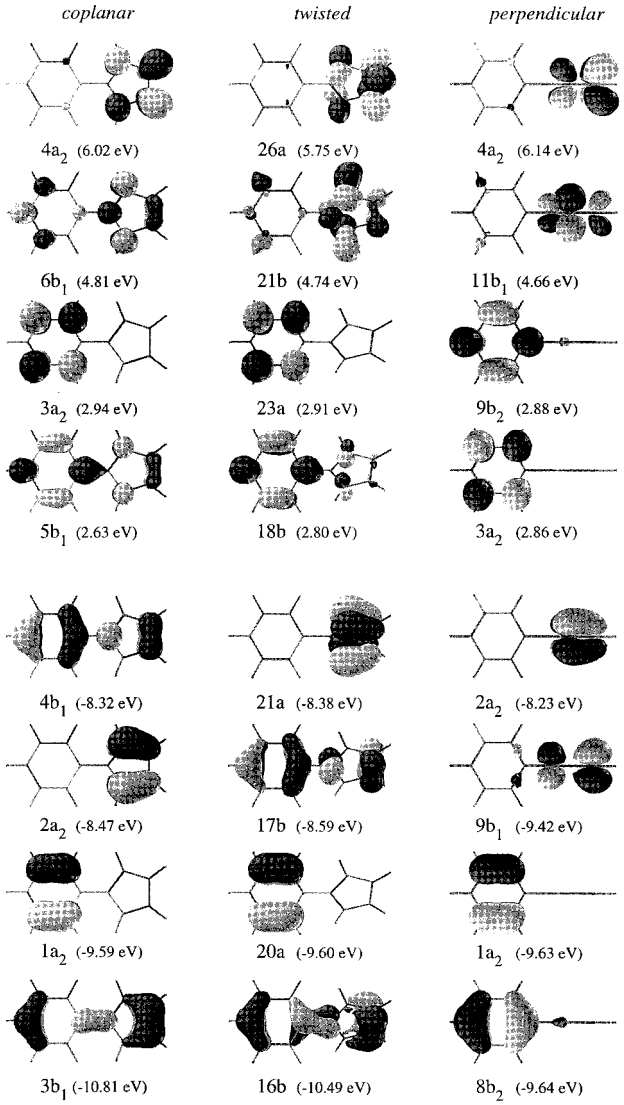

Figure 3. Highest four occupied and lowest four unoccupied π canonical MOs and SCF orbital energies computed with the ANO-type C,N[3s2pld]/H[2s] basis set.

the lowest singlet excited state, becomes actually the third excited state of twisted PHPY. The homologous 2^1B (twisted), 2^1B_2 (coplanar), and 2^1B_1 (perpendicular) are found to be close in energy, around 5.30 eV (cf. Table 3). It is consistent with the fact that the orbital energy difference between the 18b and 21a MOs (11.2 eV), LUMO and HOMO, respectively, for twisted PHPY, does not significantly vary upon the internal rotation of the system ($\Delta E(9b_2-2a_2)$(perpendicular) = $\Delta E(5b_1-2a_2)$(coplanar) = 11.1 eV). Small oscillator strength values are found for the corresponding transitions in the three conformations. Among the excited states which are computed to have a relatively large dipole moment, the 2^1B_1 perpendicular state possesses the highest value (11 D) and the lowest vertical excitation energy. Due to its CT nature, a large effect on the emission energy from the 2^1B_1 state is expected from both the geometry optimization and influence of the environment. For these reasons, the 2^1B_1 (perpendicular) state appears as the best TICT candidate. The results obtained for the emission maxima in vacuo and in acetonitrile, which shall be presented in the next section demonstrate the suitability of such proposal. The 3^1A (twisted) state correlates with the 3^1A_1 (coplanar) and 2^1A_1 (perpendicular) states. It is worth noting the pronounced increase of the oscillator strength value of the corresponding electronic transition at the coplanar structure, which might contribute to the overall shape of the absorption spectrum of PHPY around 5.7 eV.

For twisted PHPY, the transition to the 4^1A state at 5.90 eV is obtained with an oscillator strength value of 0.11, which can be related to the highest energy recorded feature.[11] The 4^1A (twisted), 4^1A_1 (coplanar), and 3^1A_1 (perpendicular) states, which are placed in the energy interval 5.9−6.1 eV, have a multiconfigurational description (cf. Table 4).

In addition, the lowest singlet state of B_2 symmetry was computed for perpendicular PHPY. Transition to the 1^1B_2 state, found at 6.02 eV, turned out to be the unique electronic transition with a non-negligible value for the oscillator strength (0.17) in the perpendicular conformation. The state is mainly described by the one-electron promotion ($2a_2 \rightarrow 11b_1$). The inspection performed on higher roots of B (twisted) and B_2 (coplanar) symmetries indicated that the correlating state of the same nature as the 1^1B_2 (perpendicular) state should be found at higher energies. The third root of B/B_2 symmetry showed instead a multiconfigurational character, involving the highest two occupied and lowest two unoccupied MOs, as expected from the one-electron diagram depicted in Figure 2. The electronic transitions to the 3^1B (twisted) and 3^1B_2 (coplanar) states (not included in Table 3) are calculated to be around 6.1 eV with small oscillator strengths values (0.03−0.05) for the corresponding electronic transitions. As pointed out above, in case

one is interested in the description of the energy region higher than 6 eV, one should bear in mind that Rydberg states are interleaved among valence states.

The observed gas-phase absorption spectrum at low temperature is characterized by two bands. The lowest energy band is broad, ranging from 4.4 to 5.5 eV, with the maximum at 4.9 eV. The highest energy band has the maximum at 6.1 eV.[11] The vertical electronic spectra computed for coplanar PHPY predicts two electronic transitions equally intense, at 4.80 and 5.6 eV, and a single transition at 6 eV for perpendicular PHPY. The coplanar and perpendicular structures can be therefore ruled out as ground-state geometries of PHPY in gas-phase. The computed results for twisted PHPY in vacuo are therefore consistent with the observed spectrum, with calculated maxima at 5.07 and 5.90 eV, in agreement with the experimental evidence. A relatively larger oscillator strength is obtained for the lowest energy transition compared to the highest-energy feature, which can be related to the actual shapes of the observed bands, broad and sharp, respectively. In view of the overall agreement between the computed spectrum of twisted PHPY and the recorded spectrum in gas phase, the present spectral information gives indirect, additional support to a nonplanar geometry of 1-phenylpyrrole in its ground state.

3.3. Emission and Nonvertical Transition Energies. Knowledge of the main changes occurring in the hypersurfaces of the ground and low-lying excited states by twisting the interring single bond is essential for the understanding of the dual fluorescence phenomenon of 1-phenylpyrrole observed in polar solvents, as well as to rationalize the reason why it is absent in the gas phase. For this purpose, geometry determinations for the relevant excited states were carried out. As described in section 2, the geometries for the ground and the considered excited states were optimized at the π-CASSCF level. The geometry so determined and the same active spaces as those used for the vertical transitions (*ext*-CASSCF) have been employed in the computation of the emission and non-vertical transition energies. A consistent comparison can therefore be performed between the computed absorption and emission spectra. The reported transitions involve the energy differences between the minima of the ground state and the excited states (0-0 absorption transition) and the vertical emission, from the excited state minima vertically to the ground state hypersurface (maximum of fluorescence in the emission band). The study includes determination of the 0-0 transition and emission maxima for the lowest excited state of coplanar (1^1B_2), twisted (1^1B), and perpendicular (1^1B_1) PHPY, and for the excited states of perpendicular PHPY with high polarity (2^1B_1 and 1^1A_2).

As expected, π-CASSCF geometry optimizations did not show any problems for the lowest root of a given symmetry employing as starting point the ground state geometry. Geometry optimizations of higher roots are, however, particularly challenging. Convergence problems were found for the second π-CASSCF root of $^1B_1$ symmetry of perpendicular PHPY. The problem was overcome by taking the optimized geometry of the 1^1A_2 (perpendicular) state as initial try, achieving the converged geometry in an efficient way. The optimized geometries for the states of interest are given in Figure 4 (1^1B (twisted)), Figure 5 (1^1B_2 (coplanar)), and Figure 6 for the perpendicular geometry (1^1B_1 (top), 2^1B_1, and 1^1A_2 (bottom)). The optimized geometries of the lowest excited state in the three conformations are characterized by C−C bond distances of the phenyl group which are about 0.03 Å longer than the aromatic standard bond length (1.40 Å, see Figure 1). This effect is due to the locally excited nature of the excited state involving mainly

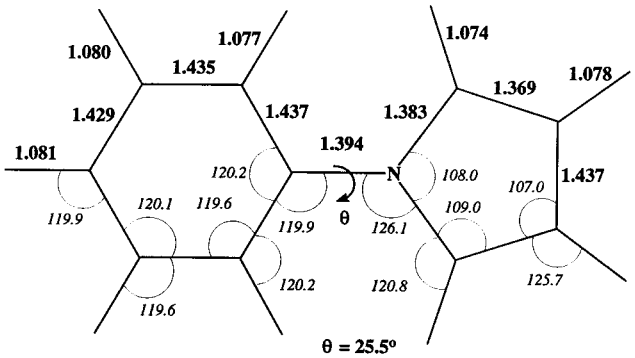

Figure 4. Geometry optimized at the π-CASSCF level for 1^1B "locally excited" (LE) state NPP. The dihedral angle between the phenyl and pyrrolic planes is denoted by θ. Bond lengths in angstroms and angles in degrees.

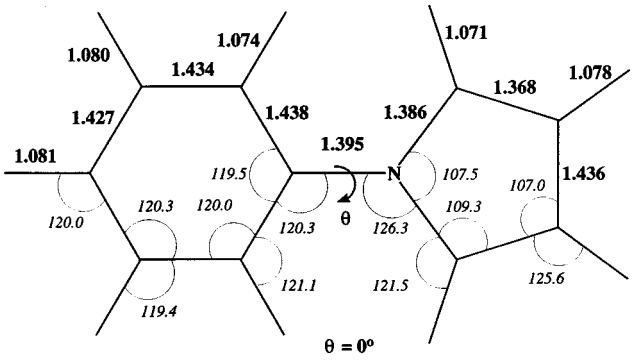

Figure 5. Geometry optimized at the π-CASSCF level for lowest-excited 1^1B_2 state of coplanar NPP. The dihedral angle between the phenyl and pyrrolic planes is denoted by θ. Bond lengths in angstroms and angles in degrees.

$\pi\pi^*$ one-electron promotions within the phenyl group. As can be seen in Figure 4, the lowest excited state is found to have a twisted form with a somewhat smaller dihedral angle between the phenyl and pyrrolic planes than the ground state ($\theta = 25.5°$ vs. 41.1°). The barrier heights to planarity and perpendicularity are estimated to be 0.05 eV (5.16 kJ/mol) and 0.28 eV (26.75 kJ/mol), respectively. The results are consistent with the derived experimental data from the electronic spectra of jet-cooled 1-phenylpyrrole. The dihedral angle $\theta = 19.8°$ and barrier heights of 1.26 kJ/mol (coplanar) and 18.26 kJ/mol (perpendicular) have been recently reported.[11] It should be noted, however, that the barrier heights determined experimentally and the present theoretical results might not be comparable. Okuyama et al.[11] have assumed in their analyses that only one excited state is responsible for the lowest-energy recorded features. The present results do not support such assumption. Geometry relaxation of the 2^1B_1 and 1^1A_2 states produces changes consistent with the π-donor and π-acceptor character of the pyrrolic and phenyl moieties, respectively. Longer interbond distances and intraring bond length alternation with respect to the ground state can be noted (see Figure 6 vs Figure 1). Thus, the trends are in accordance with the nature of the MOs involved in the description of the principal configuration of the states.

The adiabatic and emission CASPT2 electronic transitions are collected in Table 5, where for sake of comparison the transition energies computed vertically (at the ground-state geometry) are also included. In the low-energy side of the main broad absorption band, the computation predicts a weak feature placed vertically at 4.39 eV, with the origin of the band located slightly below at 4.16 eV, and a computed emission maxima at 4.07 eV. The recorded origin at 4.40 eV[11] can be related to the

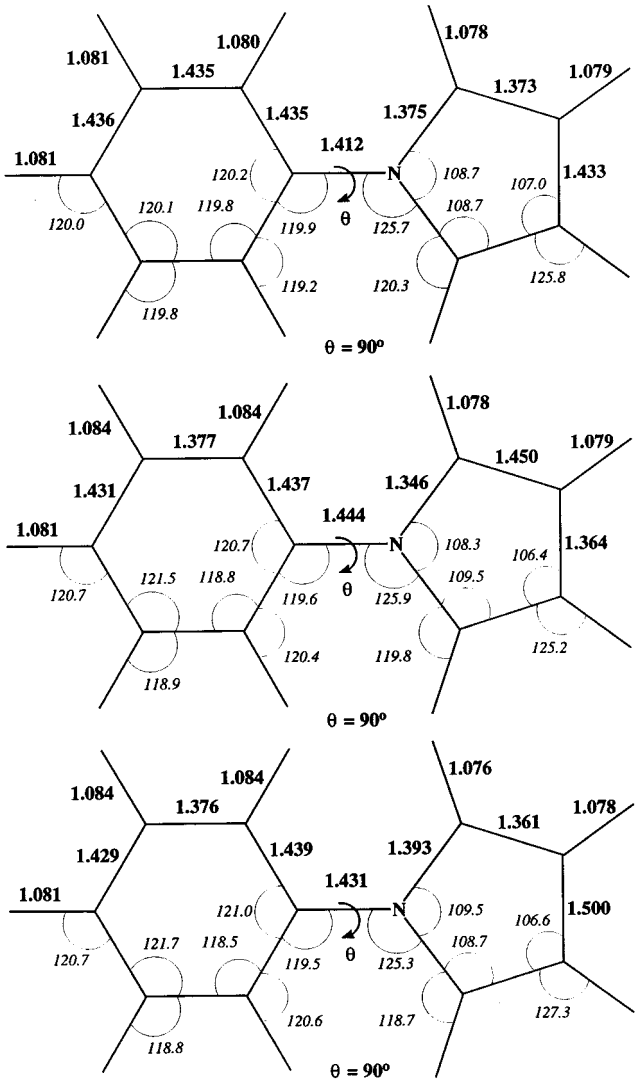

Figure 6. Geometries optimized at the π-CASSCF level for the 1^1B_1 state (top), 2^1B_1 TICT-fluorescence state (middle), and 1^1A_2 state (bottom) of perpendicular NPP. The dihedral angle between the phenyl and pyrrolic planes is denoted by θ. Bond lengths in angstroms and angles in degrees.

TABLE 5: In vacuo Computed Vertical, Adiabatic, and Emission CASPT2 Electronic Transitions (eV) for 1-Phenylpyrrole[a]

state	vertical absorption	0-0 transition	emission maxima	comments
coplanar				
1^1B_2	4.30	4.12	4.03	LE
twisted				
1^1B	4.39	4.16	4.07	LE best candidate
perpendicular				
1^1B_1	4.59	4.42	4.33	LE
2^1B_1	5.35	5.00	4.64	TICT best candidate
1^1A_2	5.89	5.57	5.38	TICT

[a] Geometries have been optimized at the π-CASSCF level with the C,N[3s2pld]/H[2s] ANO-type basis sets.

computed 0-0 transition for the 1^1B state. Two parts with different structure can be clearly seen in the fluorescence excitation spectrum (see Figure 2b in ref 11): from 4.40 eV (0-0) to near 4.5 eV and another distinct region up to 4.65 eV. The fluorescence excitation maximum at 4.65 eV (absorption maximum at 4.86 eV) could be related to the most intense electronic transition ($1^1A \rightarrow 2^1A$) predicted in vacuo at 5.07 eV.

TABLE 6: Properties at the Optimized Geometries Calculated for the LE and TICT States of 1-Phenylpyrrole in Vacuo and in Acetonitrile

	S_0 (C_2)[c]	LE (C_2)[c]	TICT (C_{2v})[c]
	In Vacuo		
dipole moment (D)	−1.51	−0.81	10.2
emission max. (eV)		4.07	4.64
exptl in *n*-heptane (eV)[a]		4.08	
	Acetonitrile[b]		
Dipole moment (D)		−1.14	13.4
Emission max. (eV)		4.07	3.72
exptl (eV)[a]		4.05	3.65

[a] Emission maxima taken from ref 9. [b] Simulated at the *ext*-CASSCF-RF/CASPT2 level. [c] Symmetry in parentheses.

The emission maxima for the TICT states 2^1B_1 and 1^1A_2 are placed at 4.64 eV and 5.38 eV. It is unlikely that solvent effects would compensate the energy difference (0.74 eV) between the two states. Therefore, the 2^1B_1 (perpendicular) appears as the lowest energy TICT candidate. In order to determine in a qualitative way the influence of solvent effects on the computed emission maxima of the LE and TICT best candidates obtained in vacuo, the environment has been simulated by introducing a self-consistent reaction field model (see section 2). Acetonitrile was selected to be the solvent. In gas phase, the emission maxima for the corresponding states (see Table 6) were computed at 4.07 and 4.64 eV from the LE and TICT states, respectively. The single fluorescence band observed in *n*-heptane[9] with a maximum at 4.08 eV agrees with the calculated result at the CASPT2 level for the LE state. The values of the dipole moments of the computed states in vacuo are quite different from each other: LE (−0.81 D) and TICT (10.2 D). Taking into account the relatively higher dipole moment of the TICT state with respect to the ground state (10.2 D vs −1.51 D), a larger stabilization of the TICT state can be expected in a polar solvent like acetonitrile, leading to a pronounced red shift of the corresponding emission maximum. The inclusion of the reaction field confirms the prediction. While the computed LE emission remains at the same energy, 4.07 eV, the calculated TICT emission drops to 3.72 eV. The large effect on the value of the fluorescence energy is a consequence of the charge transfer character of the electronic transition from the TICT to the ground state. In the CASSCF-RF/CASPT2 simulation, the excited state has been taken as initial state and the ground state (at the excited state geometry) as the final state of the promotion. The low-lying emission maximum of PHPY is computed at the CASSCF-RF/CASPT2 level to be 3.72 eV, in agreement with the observed datum in acetonitrile.[9]

The obtained results confirm therefore the suggested LE (1^1B twisted) and TICT (2^1B_1 perpendicular) states in vacuo as the responsible of the dual fluorescence phenomenon observed for PHPY in polar solvents. The results also rationalize the lack of the lowest-energy emission (A fluorescence) in gas phase, due to the occurrence of an energy barrier in the S_1 hypersurface. However, the high polarity of the TICT state favors its stabilization in polar solvents to such a large extent that the TICT state becomes the lowest excited state at the perpendicular conformation. It implies that the S_1 hypersurface from the twisted to the perpendicular structure has no enerrgy barrier in polar solvents. The nature of the S_1 state changes through the photoadiabatic reaction path, similarly as in DMABN.[21]

4. Summary and Conclusions

We have presented results of an ab initio investigation on the absorption and emission electronic spectra of 1-phenylpyr-

role. The study has been performed with multiconfigurational second-order perturbation theory using the CASPT2 method.

The geometry of the ground state and the low-lying excited states for the coplanar, twisted, and perpendicular conformations were optimized at the π-CASSCF level. Both the ground and the lowest excited state have a twisted structure, with a dihedral angle between the planes of the rings of 41.1° and 25.5°, respectively. The results are consistent with the most recent experimental determinations. From the comparison between the computed absorption spectra in vacuo of the three considered conformations and the observed spectra in the vapor one can also conclude that the ground state geometry of the system is actually twisted. For the lowest-energy band there is agreement between the transition energy (5 eV) computed with a relatively large oscillator strength and the recorded band maximum (4.9 eV) in gas phase. Interestingly, a weak feature is predicted to be hidden, with a vertical excitation energy around 4.4 eV, in the low-energy side of the main broad absorption band, which involves the lowest excited state and has been identified as the "locally excited" (LE) state.

Whether the 1-phenylpyrrole system can be considered as a TICT problem or not has been the major underlying reason to undertake the present study. Theory clearly confirms "Yes", 1-phenylpyrrole is a TICT problem. In vacuo the emission maximum from the LE state is placed at 4.07 eV, consistent with the experimental datum in a non-polar solvent like *n*-heptane (4.08 eV). In a polar solvent like acetonitrile, however, a "twisted intramolecular charge transfer" (TICT) state is stabilized to such a large extent that it becomes the lowest excited state, with a calculated emission maximum of 3.72 eV in agreement with the experimental observation at 3.65 eV. The emission maximum from the LE state, computed at 4.07 eV in acetonitrile, remains therefore unchanged in a polar environment, which can be related to the lower polarity of the LE state with respect to the TICT state of high dipole moment (around 13 D in acetonitrile).

The information obtained in the different regions of the hypersurfaces is consistent with the following view. Initially, absorption at the ground state (twisted) geometry occurs. The electronic transition to the S_2 state will carry most of the excitation energy due to its strongly dipole-allowed Franck-Condon character. A nonradiative deactivation to the S_1 (LE) state can then happen. Subsequently, the "normal" emission from the LE state takes place (B fluorescence). The character of the S_1 state progressively changes from the initial LE state to the final TICT state in polar solvents, from which the additional emission occurs (A fluorescence). In gas phase and nonpolar solvents, the photoadiabatic process is hindered by the shape of the hypersurface of the lowest excited state, with a pronounced barrier to reach the TICT state. Consequently, only fluorescence from the LE state is observed.

Acknowledgment. B.P. acknowledges financial support from Sfb 337 founded by the DFG and the European Network "Transfer and Localization of Hydrogen". The research reported in this paper has been performed within the framework of the DGES Project PB97-1377 of Spain and of the European Commission TMR network contract ERB FMRX-CT96-0079 (Quantum Chemistry for the Excited State).

References and Notes

(1) Klessinger, M.; Michl, J. *Excited States and Photochemistry of Organic Molecules.* VCH Publishers, Inc., 1995.

(2) Grabowski, Z. R.; Rotkiewicz, K.; Siemiarczuk, A.; Cowley, D. J.; Baumann, W. *Nouv. J. Chim.* **1979**, *3*, 443.

(3) Rettig, W. Photoinduced Charge Separation via Twisted Intramolecular Charge Transfer States. In *Electron Transfer I*; Mattay, J., Ed.; Topics in Current Chemistry 169; Springer: New York, 1994; p 253.

(4) Sobolewski, A. L.; Domcke, W. *Chem. Phys. Lett.* **1996**, *250*, 428.

(5) de Lange, M. C. C.; Leeson, D. T.; van Kujik, K. A. B.; Huizer, A. H.; Varma, C. A. G. O. *Chem. Phys.* **1993**, *174*, 425.

(6) Zachariasse, K. A.; Grobys, M.; Tauer, E. *Chem. Phys. Lett.* **1997**, *274*, 372.

(7) Scholes, G. D.; Phillips, D.; Gould, I. R. *Chem. Phys. Lett.* **1997**, *266*, 521.

(8) Rettig, W.; Marschner, F. *Nouv. J. Chim.* **1983**, *7*, 425.

(9) Sarkar, A.; Chakravorti, S. *Chem. Phys. Lett.* **1995**, *235*, 195.

(10) Lumbroso, H.; Bertin, D. M.; Marschner, F. *J. Mol. Struct.* **1988**, *178*, 187.

(11) Okuyama, K.; Numata, Y.; Odawara, S.; Suzuka, I. *J. Chem. Phys.* **1998**, *109*, 7185.

(12) Abu-Eittah, R.; Hilal, R.; El-Shall, M. S. *Appl. Spectrosc.* **1982**, *36*, 297.

(13) Fabian, W. M. F. *Z. Naturforsch.* **1987**, *42a*, 641.

(14) Fabian, W. M. F. *J. Comput. Chem.* **1988**, *9*, 369.

(15) Roos, B. O. The Complete Active Space Self-Consistent Field Method and Its Applications in Electronic Structure Calculations. In *Advances in Chemical Physics*; Lawley, K. P., Ed.; Ab Initio Methods in Quantum Chemistry II; John Wiley & Sons Ltd.: Chichester, England, 1987; Chapter 69, p 399.

(16) Andersson, K.; Malmqvist, P.-Å.; Roos, B. O.; Sadlej, A. J.; Wolinski, K. *J. Phys. Chem.* **1990**, *94*, 5483.

(17) Andersson, K.; Malmqvist, P.-Å.; Roos, B. O. *J. Chem. Phys.* **1992**, *96*, 1218.

(18) Roos, B. O.; Fülscher, M. P.; Malmqvist, P.-Å.; Merchán, M.; Serrano-Andrés, L. Theoretical Studies of Electronic Spectra of Organic Molecules. In *Quantum Mechanical Electronic Structure Calculations with Chemical Accuracy*; Langhoff, S. R., Ed.; Kluwer Academic Publishers: Dordrecht, The Netherlands, 1995; p 357.

(19) Roos, B. O.; Andersson, K.; Fülscher, M. P.; Malmqvist, P.-Å.; Serrano-Andrés, L.; Pierloot, K.; Merchán, M. Multiconfigurational Perturbation Theory: Applications in Electronic Spectroscopy. In *Advances in Chemical Physics: New Methods in Computational Quantum Mechanics*; Prigogine, I.; Rice, S. A., Eds.; John Wiley & Sons: New York, 1996; Vol. XCIII:219.

(20) Merchán, M.; Serrano-Andrés, L.; Fülscher, M. P.; Roos, B. O. Multiconfigurational Perturbation Theory Applied to Excited States of Organic Compounds. In *Recent Advances in Multireference Methods*; Hirao, K., Ed.; World Scientific Publishing Company: Amsterdam, 1999; Vol. 4, p 161.

(21) Serrano-Andrés, L.; Merchán, M.; Roos, B. O.; Lindh, R. *J. Am. Chem. Soc.* **1995**, *117*, 3189.

(22) Rubio, M.; Merchán, M.; Ortí, E. *Theor. Chim. Acta* **1995**, *91*, 17.

(23) Rubio, M.; Merchán, M.; Ortí, E.; Roos, B. O. *Chem. Phys. Lett.* **1995**, *234*, 373.

(24) Rubio, M.; Merchán, M.; Ortí, E.; Roos, B. O. *J. Phys. Chem.* **1995**, *99*, 14980.

(25) Widmark, P.-O.; Malmqvist, P.-Å.; Roos, B. O. *Theor. Chim. Acta* **1990**, *77*, 291.

(26) Rubio, M.; Merchán, M.; Ortí, E.; Roos, B. O. *Chem. Phys.* **1994**, *179*, 395.

(27) Molina, V.; Merchán, M.; Roos, B. O. *J. Phys. Chem. A* **1997**, *101*, 3478.

(28) Roos, B. O.; Andersson, K. *Chem. Phys. Lett.* **1995**, *245*, 215.

(29) Roos, B. O.; Andersson, K.; Fülscher, M. P.; Serrano-Andres, L.; Pierloot, K.; Merchán, M.; Molina, V. *J. Mol. Struct. (Theochem)* **1996**, *388*, 257.

(30) Malmqvist, P.-Å. *Int. J. Quantum Chem.* **1986**, *30*, 479.

(31) Malmqvist, P. Å.; Roos, B. O. *Chem. Phys. Lett.* **1989**, *155*, 189.

(32) Serrano-Andrés, L.; Fülscher, M. P.; Karlström, G. *Int. J. Quantum Chem.* **1997**, *65*, 167.

(33) Andersson, K.; Blomberg, M. R. A.; Fülscher, M. P.; Karlström, G.; Lindh, R.; Malmqvist, P.-Å.; Neogrády, P.; Olsen, J.; Roos, B. O.; Sadlej, A. J.; Schütz, M.; Seijo, L.; Serrano-Andrés, L.; Siegbahn, P. E. M.; Widmark, P.-O. *MOLCAS Version 4.0*; Department of Theoretical Chemistry, Chemical Center; University of Lund: P.O. Box 124, S-221 00 Lund, Sweden, Lund, 1997.